Free vibrations of inclined arches using finite elements

Somchai Chucheepsakul† and Wasuroot Saetiew‡

*Department of Civil Engineering, King Mongkut's University of Technology Thonburi,
Bangkok 10140, Thailand*

Abstract.   This paper presents a finite element approach for determining the natural frequencies for planar inclined arches of various shapes vibrating in three-dimensional space. The profile of inclined arches, represented by undeformed centriodal axis of cross-section, is defined by the equation of plane curves expressed in the rectangular coordinates which are : circular, parabolic, sine, elliptic, and catenary shapes. In free vibration state, the arch is slightly displaced from its undeformed position. The linear relationship between curvature-torsion and axial strain is expressed in terms of the displacements in three-dimensional space. The finite element discretization along the span length is used rather than the total arc length. Numerical results for arches of various shapes are given and they are in good agreement with those reported in literature. The natural frequency parameters and mode shapes are reported as functions of two nondimensional parameters: the span to cord length ratio (e) and the rise to cord length ratio (f).

Key words: finite elements; free vibrations; inclined elastic arches; mode shapes.

1. Introduction

A considerable amount of research work has been done on the problem of free vibrations of arches and curved beams over the past several decades. In the literature, most of the research work is limited to arches supported at same level, and the analyses have been done only in a single plane: either in-plane or out-of-plane motion. Analytical solution for free vibrations can be found in cases where arches have simple geometry. For more complex configurations, a numerical method such as finite element method may be used. In-plane vibration analysis of circular arches were reported by Den Hartog (1928), Wolf (1971), Veletsos *et al.* (1972), Austin and Veletsos (1973), Irie *et al.* (1983) and Wilson *et al.* (1994). Arches with variable curvature (non-circular geometries) had been studied by many researchers, including, Volterra and Morell (1960, 1961a), Wang (1972), Romanelli and Laura (1972), Lee and Wilson (1989) and Oh *et al.* (1999). Free vibration of planar catenary arch with unsymmetric axes was reported by Wilson and Lee (1995). Circular arches and curved beams vibrating out-of-plane were reported by Culver (1967), Shore and Chaudhuri (1972), Volterra and Morell (1961b), and Irie *et al.* (1980, 1982a, 1982b).

Although the analysis of arches and curved structures using the finite element method has been well established, it does not take advantage of arch geometry. In many practical cases, arch

---

† Professor
‡ Graduate Student

geometry can be defined by the equation of plane curves in rectangular coordinates. With this information, it is more convenient to use the present procedure to solve the problem of planar inclined arch vibrating in three-dimensional space. In the procedure, geometry of the arch is represented by the undeformed centroidal axis of cross section and defined by equation of plane curves expressed in rectangular coordinates. In the vibration state, where the arch is slightly displaced from its undeformed position, the linear relationship between curvature-torsion and axial strain is expressed in terms of displacements in three-dimensional space. In the finite element formulation, the displacements causing bending, torsion and axial deformations along its curved axis are approximated by cubic polynomials in terms of the arc length parameters. The effects of shear deformation, rotatory inertia and warping are not considered in the present paper. In the discretizing process, the span length of the arch rather than total arc length is subdivided into a number of elements since, from the architectural point of view, span length is usually known or given, but the total arc length may not. Together with the arch geometry information, input data can be reduced and alleviated. The stiffness and mass matrices are formulated to obtain the natural frequencies and corresponding mode shapes of free vibrations. Numerical results of the test problems are presented and compared favorably with those found in the literature. The natural frequency parameters and the corresponding in-plane and out-of-plane modes are demonstrated as functions of two geometrical parameters: the span to cord length ratio (e) and the rise to cord length ratio (f).

2. Method of analysis

The geometry of an inclined arch with a uniform cross-section is shown in Fig. 1(a). It can be represented by the equation of plane curves expressed in rectangular coordinates. For a given shape of the plane curve, span length, cord length and arch rise, every location along the curve can be determined. The equations of plane curves for various shapes of arches are as follows
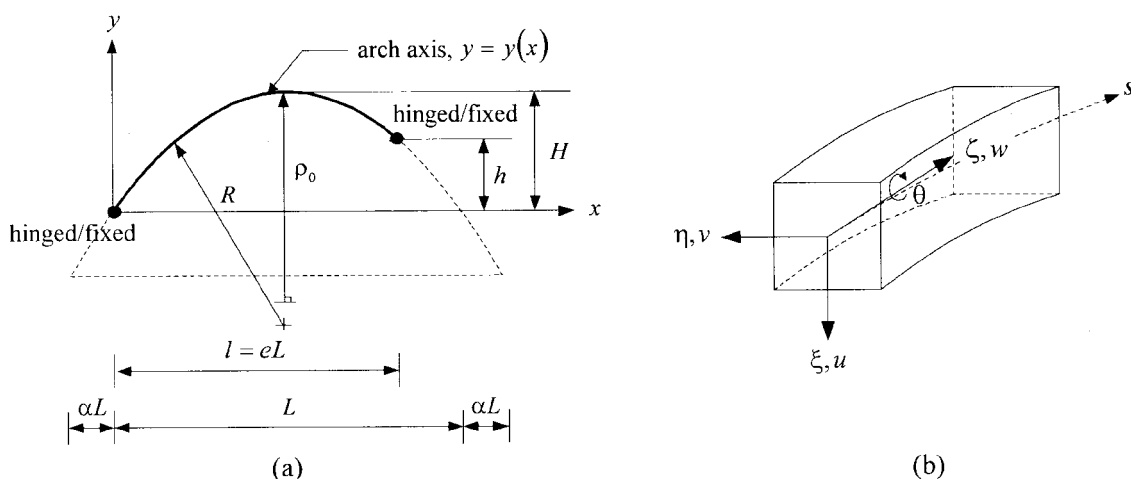

Fig. 1 (a) Arch geometry and geometric parameters; (b) coordinates at centroidal axis

2.1 Circular arch

$$y(x) = -(R - H) + \sqrt{R^2 - \left(x - \frac{L}{2}\right)^2}, \quad 0 \le x \le l \tag{1a}$$

where

$$R = \left(\frac{L^2 + 4H^2}{8H}\right), \quad H = (R + h) + \sqrt{R^2 - \left(l - \frac{L}{2}\right)^2} \tag{1b, c}$$

2.2 Parabolic arch

$$y(x) = \frac{4H}{L^2}(Lx - x^2), \quad 0 \le x \le l \tag{2a}$$

where

$$H = \frac{hL^2}{4l(L - l)} \tag{2b}$$

2.3 Sinusoidal arch

$$y(x) = H - a + a\sin(bx + b\alpha L), \quad 0 \le x \le l \tag{3a}$$

where

$$a = \frac{H}{1 - \sin(b\alpha L)}, \quad b = \frac{\pi}{L(1 + 2\alpha)} \tag{3b, c}$$

$$H = h + a - a\sin(bl + b\alpha l) \tag{3d}$$

2.4 Elliptic arch

$$y(x) = -(c - H) + \frac{c}{d}\sqrt{d^2 - \left(x - \frac{L}{2}\right)^2}, \quad 0 \le x \le l \tag{4a}$$

where

$$c = \frac{dH}{d - L\sqrt{\alpha + \alpha^2}}, \quad d = \frac{L}{2} + \alpha L \tag{4b, c}$$

$$H = (h + c) - \frac{c}{d}\sqrt{d^2 - \left(l - \frac{L}{2}\right)^2} \tag{4d}$$

2.5 Catenary arch

$$y(x) = H + \rho_0 - \rho_0\cosh\left(\frac{x - 0.5L}{\rho_0}\right), \quad 0 \le x \le l \tag{5a}$$

where

$$H = h - \rho_0 + \rho_0\cosh\left(\frac{l - 0.5L}{\rho_0}\right) \tag{5b}$$

The geometric parameters in Eqs. (1)-(5) are defined as follows, l is the span length; L is the cord length; h is the different distance of both ends supported; H is the arch rise; R is the radius of the curvature of the circular arch; α is the parameter used for identifying sinusoidal and elliptic arches only; and ρ_0 is the radius of curvature at the crown of the catenary arch which is determined by normalizing Eq. 5(a) by the catenary cord length. The non-dimensional equation of the catenary arch is defined by the shape parameters (f) and (g) as

$$\overline{y}(\overline{x}) = f + g^{-1} - g^{-1}\cosh[g(\overline{x} - 0.5)] \tag{6}$$

where

$$\overline{x} = x/L, \quad \overline{y} = y/L \tag{7a, b}$$

$$f = H/L, \quad g = L/\rho_0 \text{ (shape factors)} \tag{8a, b}$$

Substituting $\overline{x} = 1$ and $\overline{y} = 0$ into Eq. (6) leads to

$$fg - \cosh(0.5g) + 1 = 0 \tag{9}$$

For a given catenary shape factor f, the corresponding g value can be obtained from Eq. (9) using the Newton-Raphson method.

In this study it is assumed that the undeformed centroidal axis of cross-section has a shape resembling that of plane curves. Finite element discretization along the arch length, which is not yet known, may be inconvenient for the input data process, therefore, it is preferable to discretize along the span length. In the vibration state, the undeformed centroidal axis is assumed to be slightly displaced from its initial position. The ξ, η, and ζ axes form a right-handed coordinate system in normal, binomial and tangential directions, and the displacements u, v, and w at the centroidal axis corresponding to the coordinate system are shown in Fig. 1(b). The relations between curvature-torsion, strain and displacements at the deformed state for any section s along the curved centroidal axis, are obtained and given here as follows (Chucheepsakul 1989):

$$\kappa_\xi = -\frac{d^2 v}{ds^2} + \kappa\theta \tag{10a}$$

$$\kappa_\eta = \kappa + \frac{d^2 u}{ds^2} + \kappa^2 u + w\frac{d\kappa}{ds} \tag{10b}$$

$$\tau_\zeta = \frac{d\theta}{ds} + \kappa\frac{dv}{ds} \tag{10c}$$

$$\varepsilon_\zeta = \frac{dw}{ds} - \kappa u \tag{10d}$$

where κ_ξ, κ_η, and τ_ζ are the final curvatures and torsion about the ξ, η, ζ axes, respectively. θ is the rotation about the ζ-axis, ε_ζ is the axial strain and κ is the in-plane curvature of the undeformed centroidal axis and is defined as

$$\kappa = \frac{y''}{(1 + y'^2)^{3/2}} \tag{11}$$

2.6 Element strain energy and kinetic energy

Considering the eth element along the curved axis, the element strain energy, U_e, and the element kinetic energy, T_e, can be expressed as

$$U_e = \int_0^l [EA\varepsilon_\zeta^2 + EI_\xi\kappa_\xi^2 + EI_\eta(\kappa_\eta - \kappa)^2 + GJ\tau_\zeta^2]ds \tag{12}$$

$$T_e = \frac{1}{2}\int_0^l \left\{ \rho\left[\left(\frac{\partial u}{\partial t}\right)^2 + \left(\frac{\partial v}{\partial t}\right)^2 + \left(\frac{\partial w}{\partial t}\right)^2\right] + I_\rho\left(\frac{\partial \theta}{\partial t}\right)^2 \right\}ds \tag{13}$$

where EI_ξ and EI_η are the bending rigidities about ξ and η axes, GJ and EA are the torsional and axial rigidities, ρ is the mass density of arch per unit length, I_ρ is the mass polar of inertia per unit length about ζ and l is an element length measured along the curve. Eqs. (12) and (13) can be written in the following form as

$$U_e = \frac{1}{2}\int_0^l [\{\kappa^*\}^T\{E\}\{\kappa^*\} + \{\varepsilon\}^T EA\{\varepsilon\}]ds \tag{14}$$

$$T_e = \frac{1}{2}\int_0^l \{\dot{u}\}^T[\rho]\{\dot{u}\}ds \tag{15}$$

where

$$\{\kappa^*\} = \begin{Bmatrix} \kappa_\xi \\ \kappa_\eta - \kappa \\ \kappa_\zeta \end{Bmatrix}, \quad [E] = \begin{bmatrix} EI_\xi & 0 & 0 \\ 0 & EI_\eta & 0 \\ 0 & 0 & GJ \end{bmatrix}, \quad \{\varepsilon\} = \varepsilon_\zeta \tag{16-18}$$

$$\{\dot{u}\} = \begin{bmatrix} \dfrac{\partial u}{\partial t} & \dfrac{\partial v}{\partial t} & \dfrac{\partial w}{\partial t} & \dfrac{\partial \theta}{\partial t} \end{bmatrix}^T, \quad [\rho] = \begin{bmatrix} \rho & 0 & 0 & 0 \\ 0 & \rho & 0 & 0 \\ 0 & 0 & \rho & 0 \\ 0 & 0 & 0 & I_\rho \end{bmatrix} \tag{19, 20}$$

3. Finite element formulation

The displacement components u, v, w and θ of the eth element can be expressed by cubic polynomials in term of the arc length parameter s. Hence, the displacement vector $\{u\}$ can be simply expressed in terms of a nodal displacement vector $\{d\}$ through the matrix of shape functions $[F]$ as:

$$\{u\} = [F]\{d\} \tag{21}$$

in which

$$\{u\} = [u \ v \ w \ \theta]^T \tag{22}$$

The elements of 4×16 matrix $[F]$ are

$$[F] = \begin{bmatrix} f_1 \ f_2 \ 0 \ 0 \ 0 \ 0 \ 0 \ 0 \ f_3 \ f_4 \ 0 \ 0 \ 0 \ 0 \ 0 \ 0 \\ 0 \ 0 \ f_1 \ f_2 \ 0 \ 0 \ 0 \ 0 \ 0 \ 0 \ f_3 \ f_4 \ 0 \ 0 \ 0 \ 0 \\ 0 \ 0 \ 0 \ 0 \ f_1 \ f_2 \ 0 \ 0 \ 0 \ 0 \ 0 \ 0 \ f_3 \ f_4 \ 0 \ 0 \\ 0 \ 0 \ 0 \ 0 \ 0 \ 0 \ f_1 \ f_2 \ 0 \ 0 \ 0 \ 0 \ 0 \ 0 \ f_3 \ f_4 \end{bmatrix} \tag{23}$$

where the components f_1, f_2, f_3, and f_4 are the standard shape functions for a beam element (Cook 1981), and

$$\{d\} = [\ u_1 \ u_1' \ v_1 \ v_1' \ w_1 \ w_1' \ \theta_1 \ \theta_1' \ u_2 \ u_2' \ v_2 \ v_2' \ w_2 \ w_2' \ \theta_2 \ \theta_2' \ ]^T \tag{24}$$

Substitution of Eq. (21) into Eqs. (14) and (15), the strain energy and kinetic energy can be written as:

$$U_e = \frac{1}{2}\{d\}^T[k_e]\{d\} \tag{25}$$

$$T_e = \frac{1}{2}\{\dot{d}\}^T[m_e]\{\dot{d}\} \tag{26}$$

in which $\{\dot{d}\}$ is the nodal velocity vector, and $[k_e]$ and $[m_e]$ are the element stiffness and element mass matrices, written respectively as:

$$[k_e] = \int_0^l [G]^T[[A]^T[E][A] + [P]^T EA[P]][G]ds \tag{27}$$

$$[m_e] = \int_0^l [F]^T[\rho][F]ds \tag{28}$$

where matrices $[G]$, $[A]$ and row matrix $[P]$ are as follows:

$$[G] = \begin{bmatrix} f_1 & f_2 & 0 & 0 & 0 & 0 & 0 & 0 & f_3 & f_4 & 0 & 0 & 0 & 0 & 0 & 0 \\ f_1' & f_2' & 0 & 0 & 0 & 0 & 0 & 0 & f_3' & f_4' & 0 & 0 & 0 & 0 & 0 & 0 \\ f_1'' & f_2'' & 0 & 0 & 0 & 0 & 0 & 0 & f_3'' & f_4'' & 0 & 0 & 0 & 0 & 0 & 0 \\ 0 & 0 & f_1' & f_2' & 0 & 0 & 0 & 0 & 0 & 0 & f_3' & f_4' & 0 & 0 & 0 & 0 \\ 0 & 0 & f_1'' & f_2'' & 0 & 0 & 0 & 0 & 0 & 0 & f_3'' & f_4'' & 0 & 0 & 0 & 0 \\ 0 & 0 & 0 & 0 & f_1 & f_2 & 0 & 0 & 0 & 0 & 0 & 0 & f_3 & f_4 & 0 & 0 \\ 0 & 0 & 0 & 0 & f_1' & f_2' & 0 & 0 & 0 & 0 & 0 & 0 & f_3' & f_4' & 0 & 0 \\ 0 & 0 & 0 & 0 & 0 & 0 & f_1 & f_2 & 0 & 0 & 0 & 0 & 0 & 0 & f_1 & f_2 \\ 0 & 0 & 0 & 0 & 0 & 0 & f_1' & f_2' & 0 & 0 & 0 & 0 & 0 & 0 & f_3' & f_4' \end{bmatrix} \tag{29}$$

$$[A] = \begin{bmatrix} 0 & 0 & 0 & 0 & -1 & 0 & 0 & \kappa & 0 \\ \kappa^2 & 0 & 1 & 0 & 0 & \kappa' & 0 & 0 & 0 \\ 0 & 0 & 0 & \kappa & 0 & 0 & 0 & 0 & 1 \end{bmatrix} \tag{30}$$

$$[P] = [-\kappa \ 0 \ 0 \ 0 \ 0 \ 0 \ 1 \ 0 \ 0] \tag{31}$$

Here 'prime' denotes the derivative with respect to s.

Because of discretizing along the x coordinate, before the element matrices are evaluated, the variables in term of s are required to be expressed in term of x by the following relation:

$$ds = \sqrt{1 + y'^2}\, dx \tag{32}$$

Therefore, the derivative terms with respect to s can be changed to x by the relation:

$$\frac{d(\ )}{ds} = \frac{1}{\sqrt{1 + y'^2}} \frac{d(\ )}{dx} \tag{33}$$

After the element stiffness and mass matrices are evaluated they are assembled to the global system. Hence, the global equations of motion for free vibration are:

$$[K]\{D\} = \omega^2 [M]\{D\} \tag{34}$$

where $[K]$ and $[M]$ are global stiffness and mass matrices, $\{D\}$ is a mode shape vector, and ω is the natural frequencies of vibrations. The boundary conditions are as follows:

(a) hinged-hinged arches:

$$u = v = w = \theta = 0, \text{ at the left end } (x = 0) \text{ and the right end } (x = l) \tag{35}$$

(b) hinged-fixed arches:

$$u = v = w = \theta = 0, \text{ at the left end } (x = 0) \tag{36a}$$

$$u = u' = v = v' = w = w' = \theta = \theta' = 0, \text{ at the right end } (x = l) \tag{36b}$$

(c) fixed-hinged arches:

$$u = u' = v = v' = w = w' = \theta = \theta' = 0, \text{ at the left end } (x = 0) \tag{37a}$$

$$u = v = w = \theta = 0, \text{ at the right end } (x = l) \tag{37b}$$

(d) fixed-fixed arches:

$$u = u' = v = v' = w = w' = \theta = \theta' = 0, \text{ at the left end } (x = 0) \text{ and the right end } (x = l) \tag{38}$$

Gaussian quadrature numerical integration with four points is used to calculate the stiffness and mass matrices, and a standard inverse vector iteration (Bathe and Wilson 1976) is used to solve Eq. (34).

4. Numerical results and comments

A Fortran computer program based on the procedure described above was developed for determining the natural frequencies and the corresponding mode shapes. Test examples of arch problems are used to demonstrate the validity of the model formulation. The total number of span elements used throughout this analysis is twenty elements. For ease of calculation, the arches having uniform prismatic cross section and two axes of symmetry are used. The material properties of arches are as follows: cross-section area $A = 1.2 \times 10^{-3}$ m^2, mass per unit length $\rho = 9.42$ kg/m, moment of inertia $I_\xi = I_\eta = 1.2 \times 10^{-7}$ m^4, torsional constant $J = 2.02464 \times 10^{-7}$ m^4, elastic modulus $E = 210 \times 10^9$ N/m^2, shear modulus $G = 81 \times 10^9$ N/m^2. Table 1 shows the numerical comparison of frequency parameter C_{ni} for the in-plane mode of various arch shapes whereas Table 2 shows the

Table 1 Comparison of frequency parameter C_{ni} for in-plane mode

Geometry of arch	(ni)	Frequency parameter, C_{ni}				Mode shape[#]
		This study	Veletsos et al. (1972)	Lee and Wilson (1989)	Wilson and Lee (1995)	
Circular	1	27.50	27.51	-	-	A
hinged-hinged,	2	63.79	63.80	-	-	S
$l = L = 1.0606$ m,	3	123.07	123.12	-	-	A
$H = 0.2197$ m	4	141.56	141.52	-	-	S
Parabolic	1	36.11	-	36.52	-	A
hinged-hinged,	2	64.95	-	64.83	-	S
$l = L = 1.0$ m,	3	88.92	-	89.38	-	S
$H = 0.1$ m	4	148.64	-	-	-	A
Sinusoidal	1	28.52	-	29.35	-	N
hinged-fixed, $\alpha = 0.5$,	2	67.45	-	68.44	-	N
$l = L = 1.0$ m,	3	119.31	-	119.86	-	N
$H = 0.3$ m	4	149.65	-	-	-	N
Elliptic	1	20.77	-	20.88	-	A
fixed-fixed, $\alpha = 0.5$,	2	49.15	-	49.95	-	S
$l = L = 1.0$ m,	3	85.68	-	85.79	-	A
$H = 0.5$ m	4	128.28	-	-	-	S
Catenary	1	45.02	-	-	46.32	A*
hinged-hinged,	2	107.44	-	-	107.79	S*
$l = 0.75$ m , $L=1.0$ m,	3	166.83	-	-	166.51	S*
$H = 0.3$ m	4	203.69	-	-	204.21	A*
Catenary	1	73.18	-	-	72.21	A*
fixed-fixed,	2	130.99	-	-	129.23	S*
$l = 0.75$ m, $L = 1.0$ m,	3	182.39	-	-	180.57	S*
$H = 0.3$ m	4	256.94	-	-	254.69	A*

[#]A = antisymmetric; S = symmetric; N = neither antisymmetric nor symmetric; A* = close fit to antisymmetric; S* = close fit to symmetric.

Table 2 Comparison of frequency parameter C_{no} for out-of-plane mode

Geometry of arch	(no)	Frequency parameter, C_{no}		Mode shape[#]
		This study	Shore and Chaudhuri (1972)	
Circular	1	5.10	5.10	S
hinged-hinged,	2	28.63	28.65	A
$l = L = 1.0606$ m,	3	68.48	68.55	S
$H = 0.2197$ m	4	124.39	124.51	A

#A = antisymmetric; S = symmetric.

out-of-plane frequency parameter C_{no} of a circular arch. The values of frequency parameters C_{ni} and C_{no} are defined as follows:

$$C_{ni} = \omega_{ni} L^2 / \sqrt{EI_\eta / \rho} \tag{39}$$

$$C_{no} = \omega_{no} L^2 / \sqrt{EI_\xi / \rho} \tag{40}$$

It can be seen that the results are in good agreement for all cases. Thus, the authors believe that the model formulation presented herein can be used for determining the natural frequencies of arches of various shapes having geometry defined by the equation plane curves expressed in the rectangular coordinates.

The results shown in Figs. 2-17 depict the values of the first four frequency parameters (C_{ni} and C_{no})
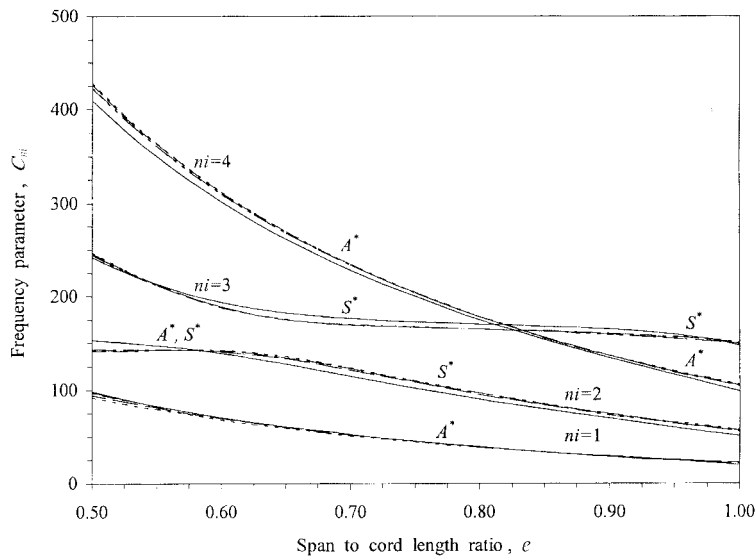
Fig. 2 Hinged-hinged arches: effect of e with $f = 0.3$ on frequency for in-plane vibration; ———, circular; ———, parabolic; ------, sinusoidal($\alpha = 0.5$); ----, elliptic($\alpha = 0.5$); ----, catenary
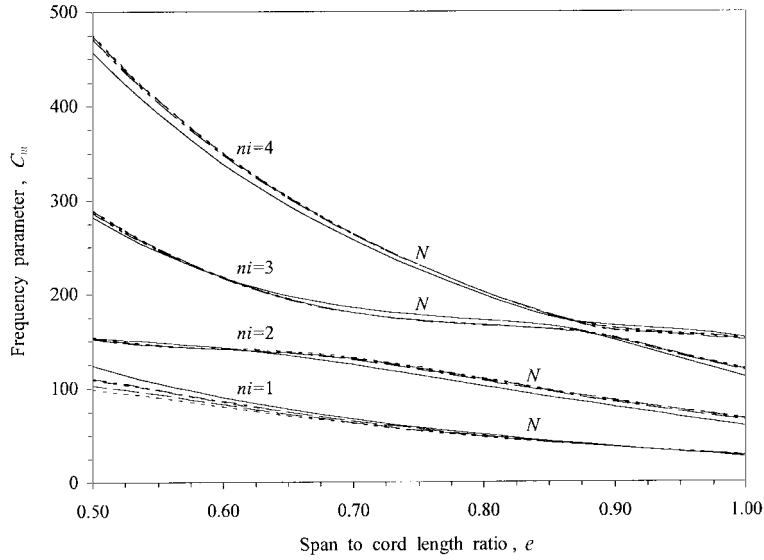
Fig. 3 Hinged-fixed arches: effect of e with $f = 0.3$ on frequency for in-plane vibration. Key as Fig. 2
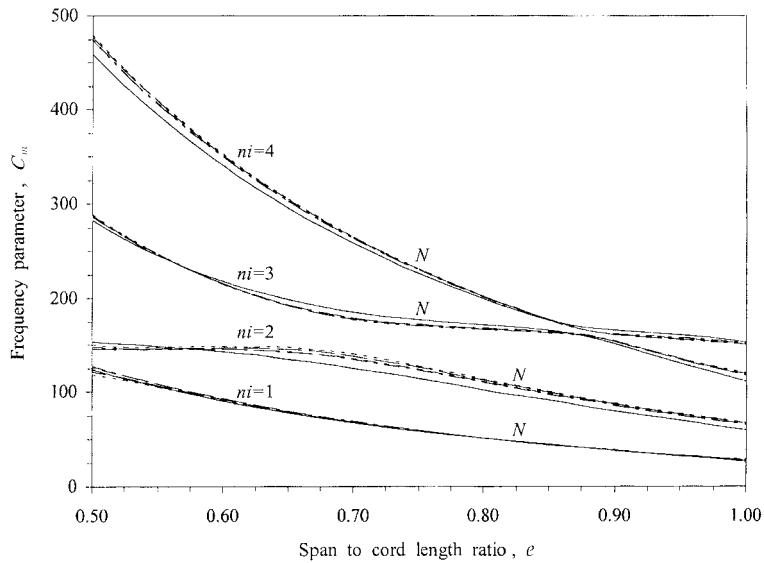
Fig. 4 Fixed-hinged arches: effect of e with $f = 0.3$ on frequency for in-plane vibration. Key as Fig. 2

corresponding to the first four free vibration modes of the five arch shapes. The hinged-hinged, hinged-fixed, fixed-hinged, and fixed-fixed end constraints were considered for each of the arch geometry with the given parameters of the span to cord length ratio (e), and the rise to cord length ratio (f) and α (it is noted here that α is used for sinusoidal and elliptic geometries only).

Figs. 2-9 show the variation of C_{ni} and C_{no} due to effect of the span to cord length ratio e with
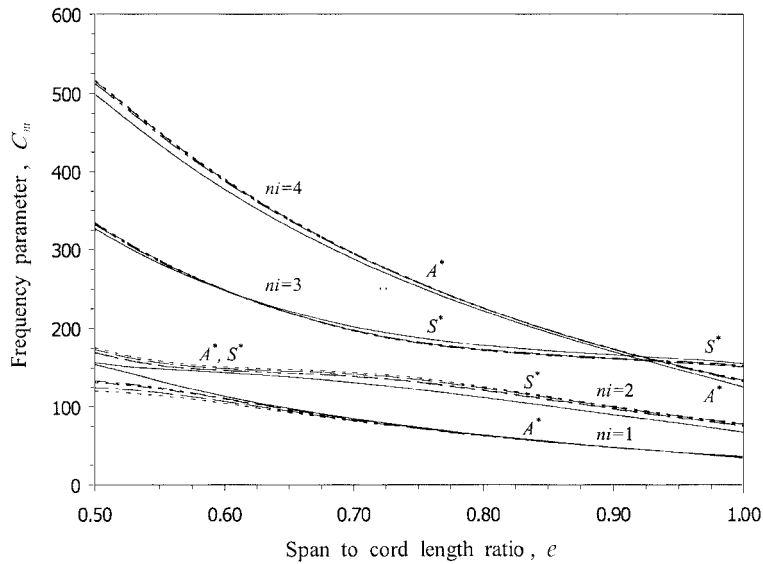
Fig. 5 Fixed-fixed arches: effect of e with $f = 0.3$ on frequency for in-plane vibration. Key as Fig. 2
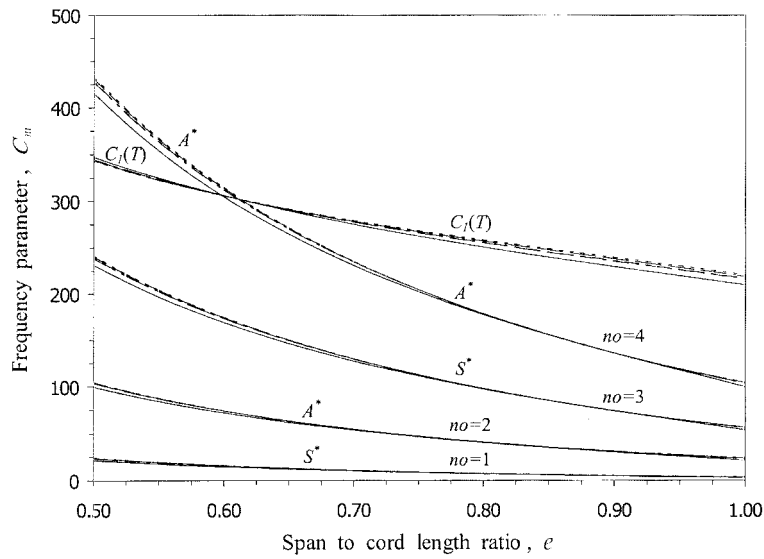
Fig. 6 Hinged-hinged arches: effect of e with $f = 0.3$ on frequency for out-of-plane vibration. Key as Fig. 2

fixed value of $f = 0.3$ and $\alpha = 0.5$. The end constraint of all five arches are varied consecutively from hinged-hinged, to hinged-fixed, to fixed-hinged, and to fixed-fixed conditions. It can be seen that each value of frequency parameter increases with the increase of constraint condition, while the other parameters remain constant. It is also observed that the frequency parameters decrease with the increase in span to cord length ratio. For in-plane vibration (Figs. 2 and 5), it appears that frequency crossover as well as modal transition occur between two mode shapes $ni = 3$ and $ni = 4$,
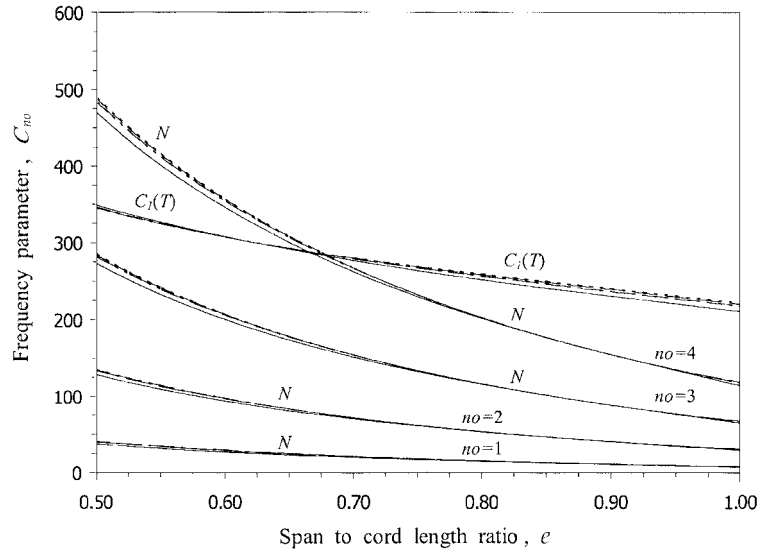
Fig. 7 Hinged-fixed arches: effect of *e* with *f* = 0.3 on frequency for out-of-plane vibration. Key as Fig. 2
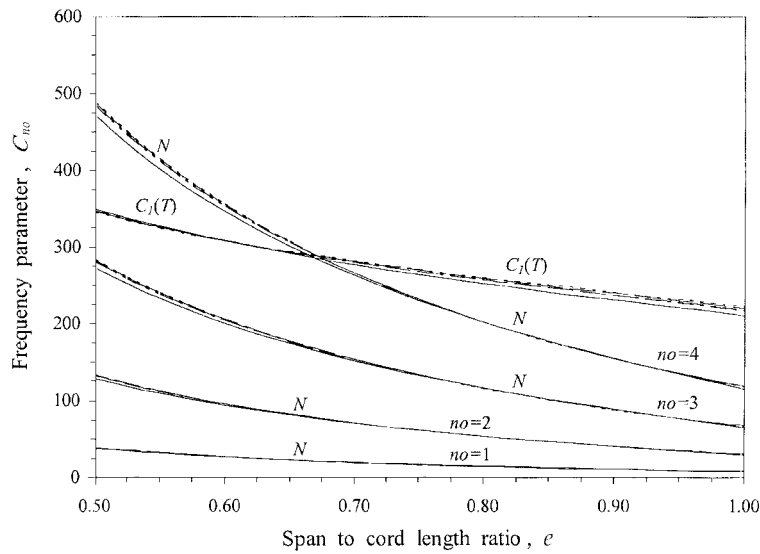
Fig. 8 Fixed-hinged arches: effect of *e* with *f* = 0.3 on frequency for out-of-plane vibration. Key as Fig. 2

except for hinged-fixed and fixed-hinged conditions in Figs. 3 and 4. The circular arch is nearly fit to symmetric mode shape at where $ni = 2$, where as the arches with variable curvature (parabolic, sinusoidal, elliptic and catenary) are nearly fit to antisymmetric and changed to symmetric mode shapes when the span to cord length ratio is increased, as shown in Figs. 2 and 5 respectively. For out-of-plane vibration (Figs. 6-9), the values of C_{no} for all arch geometries are slightly different and have the same trend. The lowest torsional frequency parameter $C_1(T)$ represented by the torsional
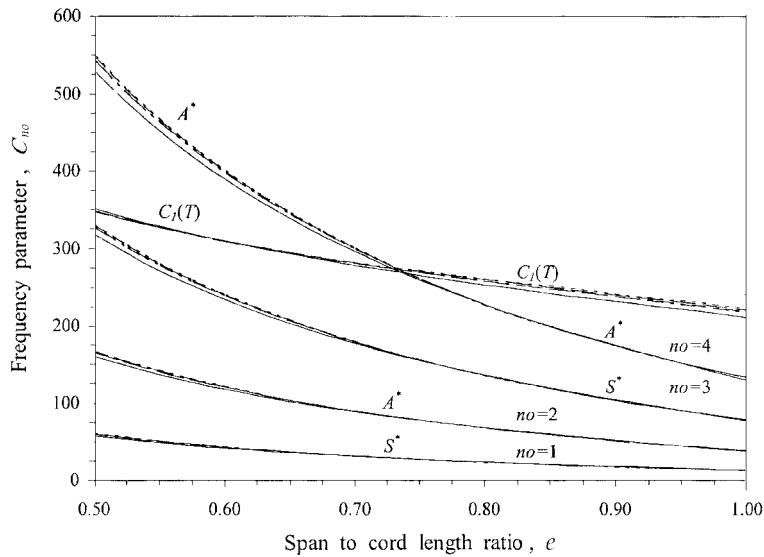
Fig. 9 Fixed-fixed arches: effect of e with $f = 0.3$ on frequency for out-of-plane vibration. Key as Fig. 2
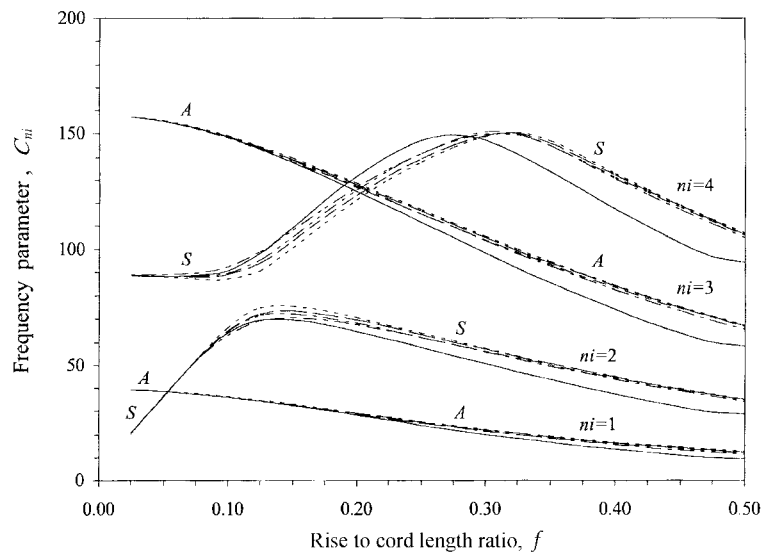
Fig. 10 Hinged-hinged arches: effect of f with $e = 1.0$ on frequency for in-plane vibration. Key as Fig. 2

angle is found and at $e = 0.5$ this value belongs to the fourth mode of vibration.

Figs. 10-17 show the variation of C_{ni} and C_{no} due to the effect of the rise to cord length ratio f with fixed value of $e = 1.0$ and $\alpha = 0.5$. The end constraint conditions are varied from hinged-hinged to hinged-fixed (or fixed-hinged) to fixed-fixed conditions for all geometry of arches. It can be seen that each value of frequency parameter increases, while other parameters remain constant (for hinged-fixed and fixed-hinged arches, the frequency parameters are equivalent due to the same end
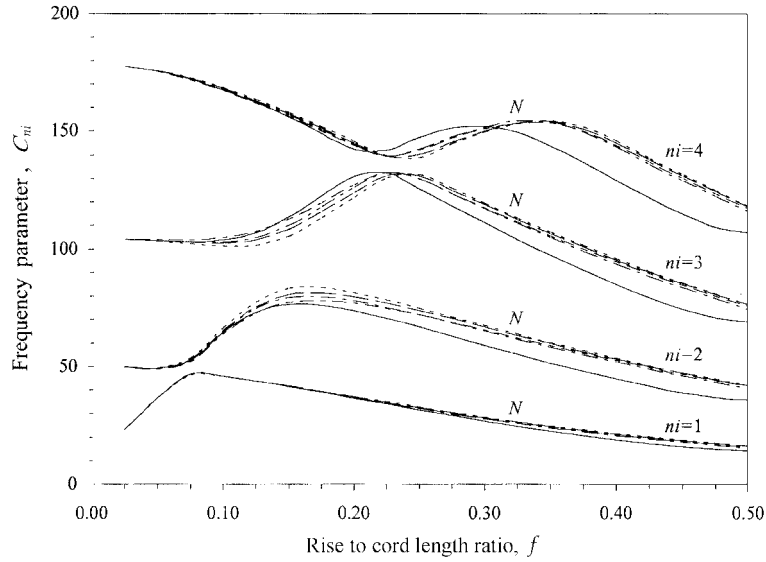
Fig. 11 Hinged-fixed arches: effect of f with $e = 1.0$ on frequency for in-plane vibration. Key as Fig. 2
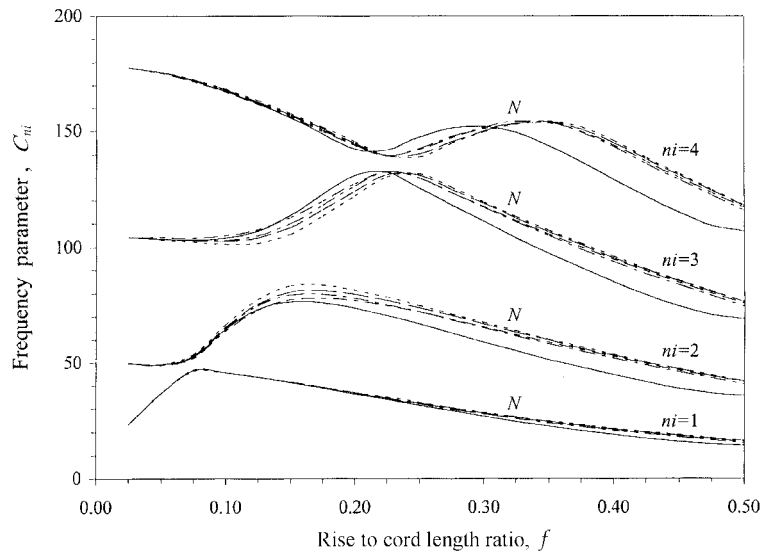

Fig. 12 Fixed-hinged arches: effect of f with $e = 1.0$ on frequency for in-plane vibration. Key as Fig. 2

constraint condition). For in-plane vibration (Figs. 10 and 13), it is observed that frequency crossover as well as modal transitions can occur between two mode shapes $ni = 1$ and $ni = 2$, $ni = 3$ and $ni = 4$, however, the frequency crossover does not occur in hinged-fixed and fixed-hinged arches as found in Figs. 11, 12. For out-of-plane vibration (Figs. 14-17), it is found typically that the frequency parameters decrease with the increasing value of rise to cord length ratio, and the mode shapes of arches with same end conditions can be identified. The mode shapes for arches with
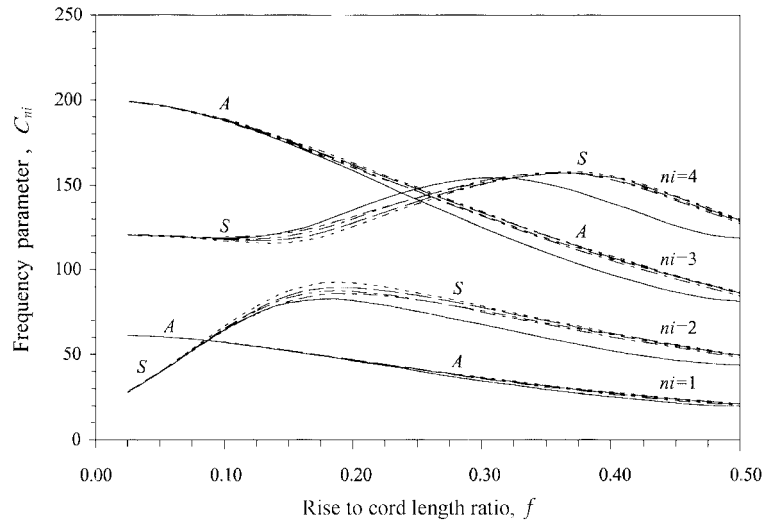
Fig. 13 Fixed-fixed arches: effect of f with $e = 1.0$ on frequency for in-plane vibration. Key as Fig. 2
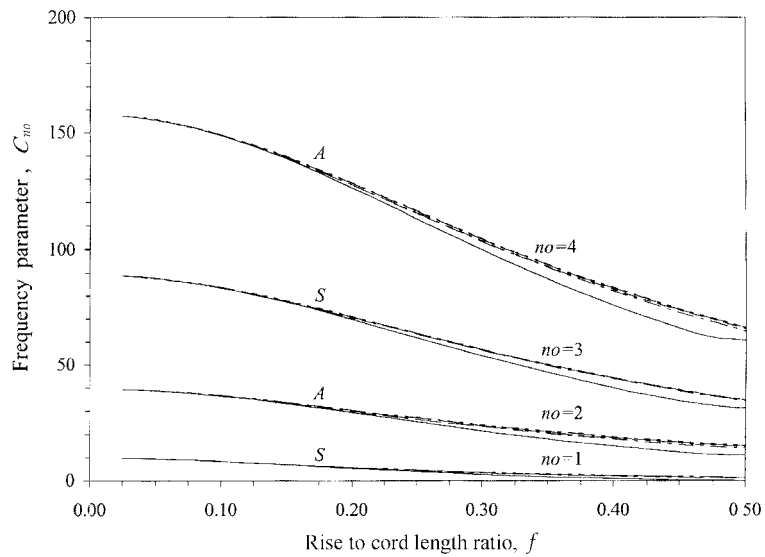

Fig. 14 Hinged-hinged arches: effect of f with $e = 1.0$ on frequency for out-of-plane vibration. Key as Fig. 2

mixed end conditions can be neither symmetric nor anti-symmetric.

5. Conclusions

A finite element procedure for free vibration analysis of the planar arches with support at the same or different level, and vibrating in three-dimensional space has been presented. The geometry
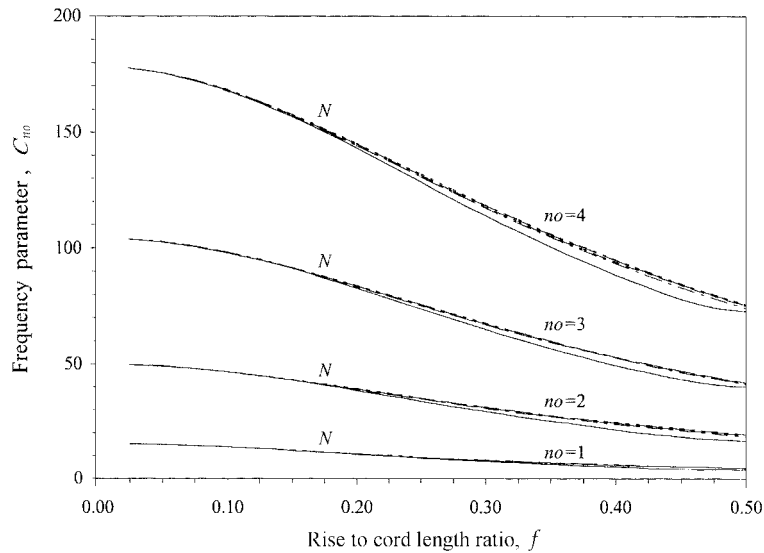
Fig. 15 Hinged-fixed arches: effect of f with $e = 1.0$ on frequency for out-of-plane vibration. Key as Fig. 2
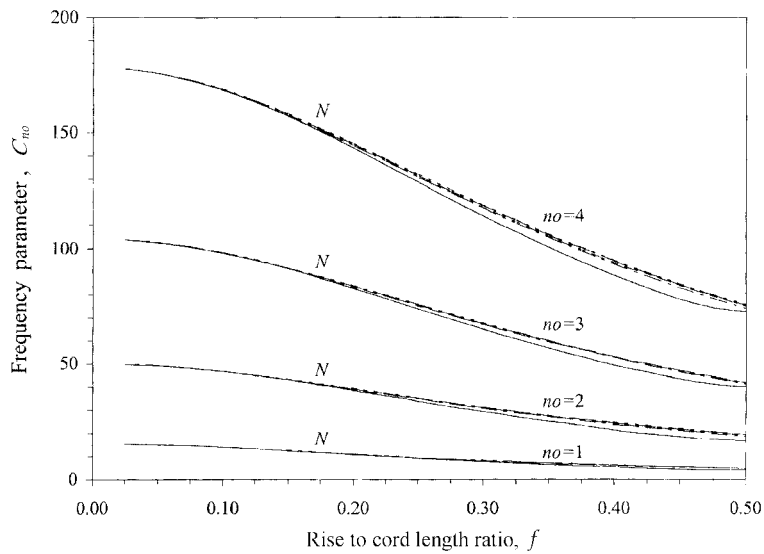

Fig. 16 Fixed-hinged arches: effect of f with $e = 1.0$ on frequency for out-of-plane vibration. Key as Fig. 2

of arches is represented by an equation of a plane curve in rectangular coordinates The model formulation has been verified by the favorable comparisons the values of the frequency parameters with those reported in the literature. For a given set of arch parameters (e and f) and matching end constrains, numerical results have shown that the frequency parameters for arches with variable curvature (parabolic, sinusoidal, elliptic and catenary arches) change only slightly in these groups; but show somewhat larger differences for the circular arch due to its constant curvature. As
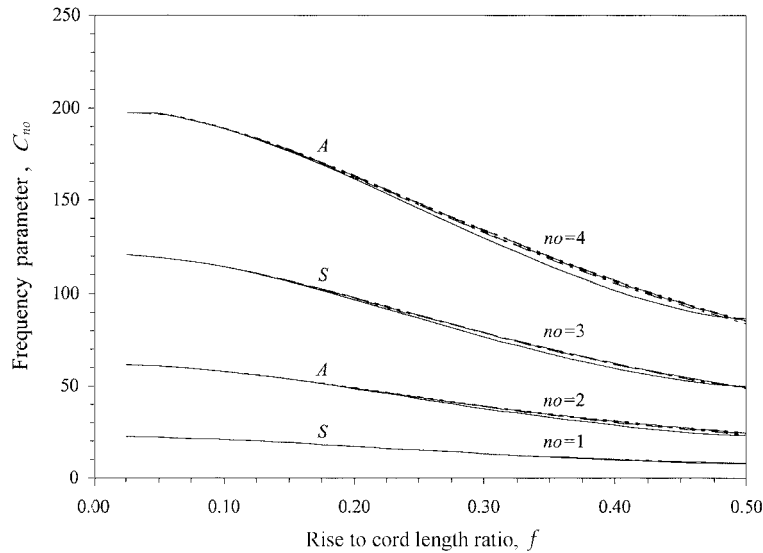
Fig. 17 Fixed-fixed arches: effect of f with $e = 1.0$ on frequency for out-of-plane vibration. Key as Fig. 2

expected, the mode shapes for the hinged-fixed and fixed-hinged cases are neither symmetric nor antisymmetric because of the difference in end conditions. For the hinged-hinged and the fixed-fixed types of arches supporting at the same level the mode shapes are found to be the alternating pattern between anti-symmetric and symmetric modes. For the hinged-hinged and the fixed-fixed end conditions of arches supporting at different levels, the numerical results have shown that neither pure symmetric nor pure antisymmetric mode shapes exist.

Acknowledgements

References

Austin, W.J. and Veletsos, A.S. (1973), "Free vibration of arches flexible in shear", *J. Eng. Mech. Div.*, ASCE, **99**(EM4), 735-753.
Bathe, K.J. and Wilson, E.L. (1976), *Numerical Methods in Finite Element Analysis*, Prentice-Hall, Inc., Englewood Cliffs, N.J.
Chucheepsakul, S. (1989), "Free vibration of elastic arches", *Proc. the Second East Asia-Pacific Conf. on Struct. Engrg. and Const.*, Chiang Mai, Thailand, 1610-1616.
Cook, R.D. (1981), *Concepts and Applications of Finite Element Analysis*, *Third Edition*, John Wiley & Sons, Singapore.
Culver, C.G. (1967), "Natural frequencies of horizonatally curved beams", *J. Struct. Div.*, ASCE, **93**(ST2), 189-203.
Den Hartog, J.P. (1928), "The lowest natural frequency of circular arcs", *Philosophical Magazine*, Series 7,

5(28), 400-408.

Irie, T., Yamada, G. and Takahashi, I. (1980), "Out-of-plane vibration of arc bar of variable cross-section", *Bulletin of the JSME*, **23**(181), 1200-1205.

Irie, T., Yamada, G. and Tanaka, K. (1982a), "Free out-of-plane vibration of arcs", *J. Appl. Mech.*, ASME, **49**, 439-441.

Irie, T., Yamada, G. and Tanaka, K. (1982b), "Natural frequencies of out-of-plane vibration of arcs", *J. Appl. Mech.*, ASME, **49**, 910-913.

Irie, T., Yamada, G. and Tanaka, K. (1983c), "Natural frequencies of in-plane vibration of arcs", *J. Appl. Mech.*, ASME, **50**, 449-452.

Lee, B.K. and Wilson, J.F. (1989), "Free vibration of arches with variable curvature", *J. Sound and Vib.*, **136**(1), 75-89.

Oh, S.J., Lee, B.K. and Lee, I.W. (1999), "Natural frequencies of non-circular arches with rotatory inertia and shear deformation", *J. Sound and Vib.*, **219**(1), 23-33.

Romanelli, E. and Laura, P.A.A. (1972), "Fundamental frequencies of non-circular, elastic, hinged arch", *J. Sound and Vib.*, **24**(1), 17-22.

Shore, S. and Chauduri, S. (1972), "Free vibration of horizontally curved beams", *J. Struct. Div.*, ASCE, **98**(ST3), 793-796.

Veletsos, A.S., Austin, W.J., Pereira, C.A.L. and Wung, S.J. (1972), "Free in-plane vibration of circular arches", *J. Eng. Mech. Div.*, ASCE, **98**(EM2), 311-329.

Volterra, E. and Morell, J.D. (1960), "A note on the lowest natural frequency of elastic arcs", *J. Appl. Mech.*, ASME, Series E, **27**(4), 744-746.

Volterra, E. and Morell, J.D. (1961a), "Lowest natural frequencies of elastic hinged arcs", *J. Acoust. Soc. Am.*, **33**(12), 1787-1790.

Volterra, E. and Morell, J.D. (1961b), "Lowest natural frequency of elastic arcs for vibrations outside the plane of initial curvature", *J. Appl. Mech.*, ASME, Series E, **28**(4), 624-627.

Wang, T.M. (1972), "Lowest natural frequency of clamped parabolic arch", *J. Struct. Div.*, ASCE, **98**(ST1), 407-411.

Wilson, J.F., Lee, B.K. and Oh, S.J. (1994), "Free vibrations of circular arches with variable cross-section", *Struct. Eng. Mech.*, **2**(4), 345-357.

Wilson, J.F. and Lee, B.K. (1995), "In-plane free vibrations of catenary arches with unsymmetric axes", *Struct. Eng. Mech.*, **3**(5), 511-525.

Wolf, J.A., Jr. (1971), "Natural frequencies of circular arches", *J. Struct. Div.*, ASCE, **97**(ST9), 2337-2350.